



---

**Research Paper / Makale**

---

**Permanent Magnet Flux Switching Torque Performance Indicator**

M. F. M. Ab HALIM<sup>1,2a\*</sup>, Erwan SULAIMAN<sup>2b</sup>

<sup>1</sup>Fakulti Teknologi Kejuruteraan Elektrik dan Elektronik, Universiti Teknikal Malaysia Melaka

<sup>2</sup>EMCenter, Faculty of Electrical and Electronic Engineering, Universiti Tun Hussein  
Onn Malaysia

\*:[mohd.firdaus@utem.edu.my](mailto:mohd.firdaus@utem.edu.my)

**Received/Geliş:** 00.00.2021

**Accepted/Kabul:** 00.00.2021

**Abstract:** Flux switching machine (FSM) offer advantages such as rotor robustness and simple driving circuit compared to competing machine. This paper attempts to process the torque, volume and current information from 35 latest Permanent Magnet (PM) FSM publication into a standardized Torque Performance Indicator (TPI), which are torque density, torque constant, torque constant density and torque-magnet ratio. The distribution median shows that torque density, torque constant, torque constant density and torque-magnet ratio are 23.24kNm/m<sup>3</sup>, 0.43Nm/A, 0.616Nkm/Am<sup>3</sup> and 30.79Nm/kg respectively. Among many design variation, outer rotor configuration produces good values as overall in the TPI. This information can be used to guide the machine designer to compare and compete based on the standardized TPI.

**Keywords:** Flux switching machine, Machine design, Torque density, Torque constant, Finite element

---

**Kalıcı Mıknatıs Akısı Anahtarlama Tork Performansı Gösterge**

**Öz:** Flux switching machine (FSM), rakip makineye kıyasla rotor sağlamlığı ve basit sürüş devresi gibi avantajlar sunar. Bu makale, tork, hacim ve akım bilgilerini en son 35 Permanent Magnet (PM) FSM yayınından, tork yoğunluğu, tork sabiti, tork sabit yoğunluğu ve tork-mıknatıs oranı olan standartlaştırılmış bir Torque Performance Indicator (TPI) işlemeye çalışmaktadır. Dağılım medyanı, tork yoğunluğu, tork sabiti, tork sabit yoğunluğu ve tork-mıknatıs oranının sırasıyla 23.24kNm / m<sup>3</sup>, 0.43Nm / A, 0.616Nkm / Am<sup>3</sup> ve 30.79Nm / kg olduğunu göstermektedir. Birçok tasarım varyasyonu arasında, dış rotor konfigürasyonu genel olarak TPI'da olduğu gibi iyi değerler üretir. Bu bilgi, makine tasarımcısına standartlaştırılmış TPI'ya göre karşılaştırma ve rekabet etme konusunda rehberlik etmek için kullanılabilir.

**Anahtar Kelimeler:** Akı anahtarlama makinesi; Makine tasarımı; Tork yoğunluğu; Tork sabiti; Sonlu elemanlar

---

**1. Introduction**

Electric car deployment has been growing rapidly over the past ten years, with the global stock of electric passenger cars passing 5 million in 2018, an increase of 63% from the previous year. About 45% of electric cars on the road in 2018 were in China compared to 39% in 2017. In comparison, Europe accounted for 24% of the global fleet, just 2% above the United States [1, 2]. In order to achieve all these market objectives, all these items related to vehicle electric drives, which include electric machines, power electronics and their respective cooling system should be improved further. Electrical machine design advancement has become competitive in recent years. According to the standard IEC line motor (IEC 60034-30-1) released in 2014, the motor efficiency level has

*How to cite this article*

M. F. M. Ab Halim, E. Sulaiman., A., "Permanent Magnet Flux Switching Torque Performance Indicators" El-Cezeri Journal of Science and Engineering, 2021, 8(2); 582-591.

*Bu makaleye atıf yapmak için*

M. F. M. Ab Halim, E. Sulaiman., "Kalıcı Mıknatıs Akısı Anahtarlama Tork Performansı Gösterge" El-Cezeri Fen ve Mühendislik Dergisi 2021, 8(2); 582-591.

ORCID ID: <sup>a</sup>0000-0001-6965-9143; <sup>b</sup>0000-0003-0303-6191

included the forth efficiency level which is IE4 namely super premium efficiency that categorize the maximum achievable efficiency to be 96.7% [3]. Nevertheless, this number hold true only for conventional type of motor that uses direct on-line operation mainly synchronous and induction motor. For EV application, the efficiency target is 94% for its drive system [4]. Meanwhile, DC motor are equally important and useful to get its due attention because of the main source of power to drive the motor is direct current that can be supplied by battery. This feature enables the motor to be used in electrical vehicle application. (Figure 1) shows the classification of dc electrical machine in commutation type and field excitation [5].

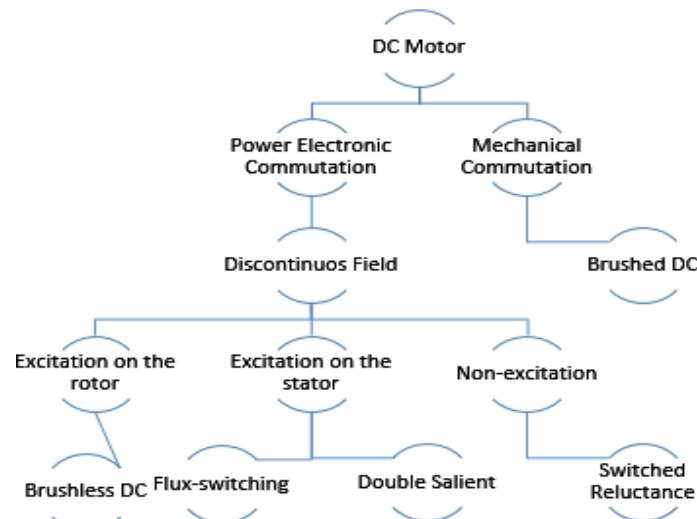


**Figure 1.** Classification of dc electrical machine

Flux switching machine (FSM) offer advantages such as rotor robustness and simple driving circuit compared to competing machine. It requires a simple converter to drive the motor and inherit robust rotor structure such in switch reluctance machine. This paper attempts to process the information from 35 latest PMFSM publication into a standard Torque Performance Indicator (TPI), which are torque density, torque constant, torque constant density and torque-magnet ratio. Among many design variation, outer rotor configuration performed reasonably well based on the overall TPI. This information can be used to guide the machine designer to compare and compete based on the standardized TPI.

## 2. Working Principle of Permanent Magnet Flux Switching Machine

Flux switching motor is a combination of the switched reluctance motor and the inductor alternator. The first PSM motor was discovered in [6] in 1999. The motivation of this invention is to introduce simplicity in motor design and power electronics controller. In a later study [7], due to rapid design evolution in the automotive industry, mechanically driven auxiliaries were being substituted by electrically driven equipment for example water pumps, steering system, heating, ventilation and air-conditioning. Brushless dc motor, induction motor and switched reluctance motor were chosen, but it comes with a relatively costly power electronic motor drive. To understand its working principle, a flux switching motor is drawn in (Figure 2a). This motor is a configuration of 8 stator slot-4rotor pole structure. The field winding coil 1 is feed with direct current continuously while the armature winding supplies DC according to the position of the rotor.

The circuit diagram for this motor is illustrated in (Figure 2b). It is important to make aware of these two figures to reflect the robustness of the motor structure and the simplicity of the motor driving circuit. (Figure 3a and 3b) illustrate the flux path at two rotor's positions. Alignment of the rotor poles and stator poles can be considered as the reference position ( $\Theta_r = 0^\circ$ ).

The flux enters from stator pole through the rotor pole and exit at the aligned stator pole 90° from the initial point. The flux path is created by the DC field F- and armature coil 2 A+ when switch S1 is at the “ON” state.

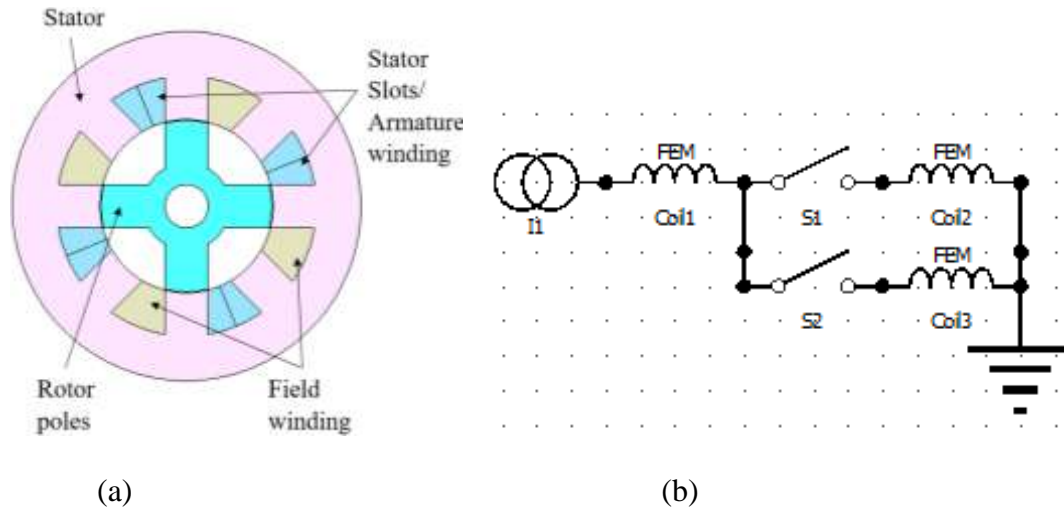


**Figure 2.** Flux switching machine structure and circuit diagram for flux switching motor 8/4 stator slot-rotor pole.

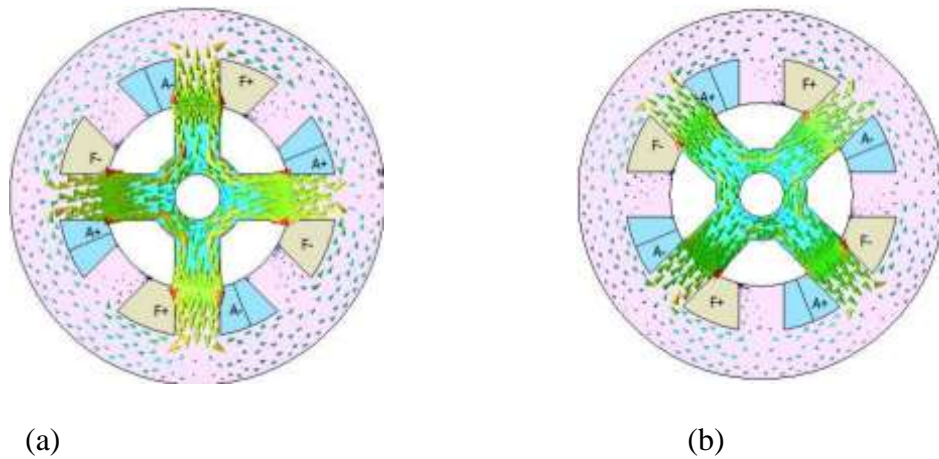


**Figure 3.** Flux direction at rotor position (a)  $\Theta_{r1} = 0^\circ$  S1 ON/S2 OFF (b)  $(\Theta_{r2} = 90^\circ)$  S1 OFF/S2 ON

At the same instant, with the field winding having a constant direct current, the polarity of armature coil 3 turns to receive the direct current (F+, a-) by switching S1 to “OFF” state and switch S2 to “ON” state. In this state, the resultant flux path is to anti-clockwise direction; hence the rotor moves anti-clockwise to the next align pole ( $\Theta_{r2} = 90^\circ$ ). This state change continues to switch the flux path by controlling the switch S1 and S2 through the bifilar winding, thereby the resultant magnetic field attracts the rotor and the continuous rotation of the motor is maintained.

### 3. PMFSM Standardized TPI Procedure and Result

#### 3.1. Torque Density and Torque Constant

Design criteria of any electrical machine mainly focus on output power and torque. However, each topology may not give the optimum torque due to its size and application. PMFSM can be categorized into four main structure, that is an inner rotor, outer rotor, double rotor and double stator. In order to understand its torque performance, power or torque output are insufficient.

Thirty-five latest publications that consist of a variety of topology were studied. Information such as motor volume, magnet volume, current, output torque from these publications were used to calculate torque density  $T_d$ , and torque constant  $T_c$ . This information should be able to assist the researcher in PMFSM to explore other regions of  $T_c$  and  $T_d$ . Even though it is unfair to group every design due to its specific application, comparing future PMFSM research against this data might be useful in general.  $T_d$ , is defined as the ratio of torque to the volume of the motor in SI units  $Nm/m^3$ . ( $T_d$ ) is calculated by using the equation 1.

$$T_d = \frac{T}{V_{ol}} \tag{1}$$

( $T_c$ ) is defined as the ratio of torque to the value of the peak armature current in  $Nm/A$  as shown in the following equation 2 [8].

$$T_c = \frac{T}{I_{ar}} \tag{2}$$

Some of the motor volume data were not available in the previous research paper. Hence, the geometry was redrawn according to the figure provided in the research paper. The total volume of the machine was calculated by subtracting air-gap volume between the rotor pole and shaft. The PM density used in calculating PM weight or volume is set to  $7550kg/m^3$  which is NdFeb type having a strength of the magnetic field  $B_r$  between 1 to 1.4 T. The largest volume found from 35 PMFSM designs is around  $0.006m^3$ . Figure 4 shows the torque density versus motor volume graph and Figure 5 shows the torque constant versus motor volume.

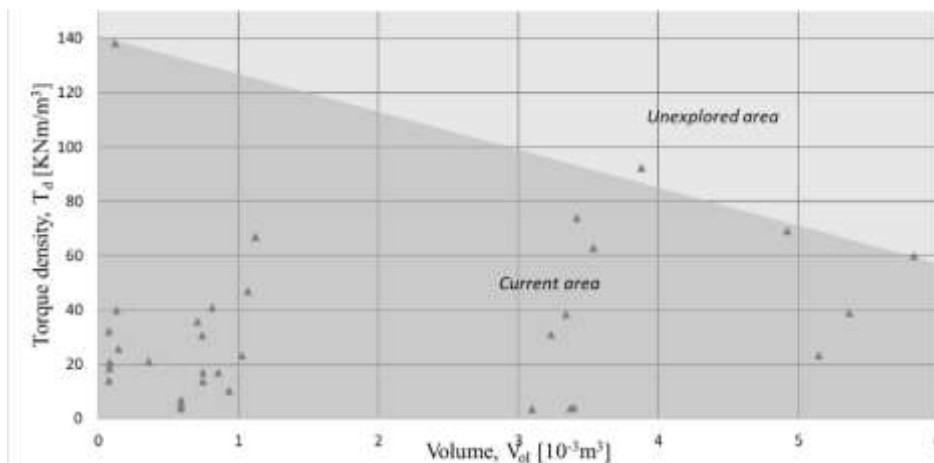


**Figure 4.** Torque density ( $T_d$ ) versus volume (Vol) from past PMFSM publication.

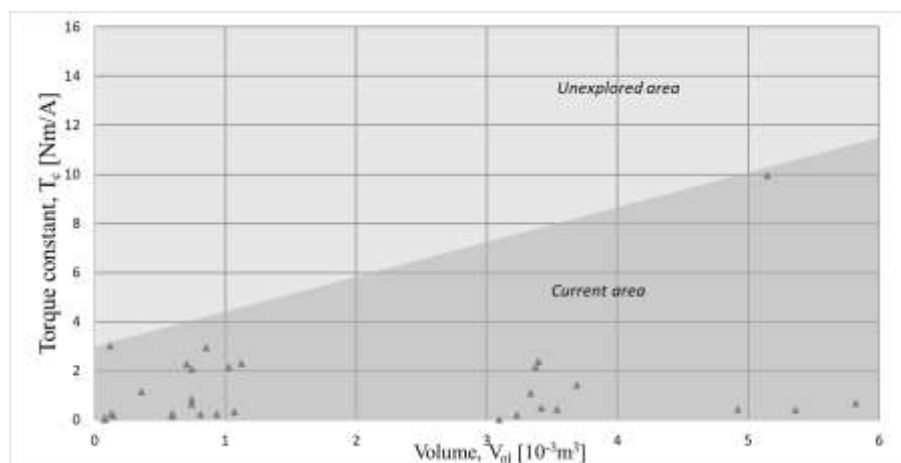


**Figure 5.** Torque constant ( $T_c$ ) versus volume (Vol) from past PMFSM publication

### 3.2. Torque Constant Density and Torque-Magnet Ratio

Based on (Figure 4) and (Figure 5), limited design has been performed in the volume region around  $0.002 \text{ m}^3$ . A correctly size PMFSM could enable significant improvements in performance and cost, thus representing a critical knowledge that every designer should take into consideration [9]. The highest torque density,  $T_d$  is  $138.11 \text{ KNm/m}^3$  while torque constant,  $T_c$  is  $9.967 \text{ Nm/A}$ .  $T_d$  is the ratio of mechanical torque over the physical size of an active part in the motor. At the same time,  $T_c$  is the ratio of electrical energy (current) being converted into mechanical energy. Although the PMFSM in the literature currently has high  $T_d$  and  $T_c$ , portable application demands higher  $T_d$  and  $T_c$ .

To obtain alternative TPI, both parameters of  $T_d$  and  $T_c$  are rearranged as shown in equation 3 ( $T_{cd}$ ). The fourth TPI is proposed in equation 4 ( $T_{mag}$ ). This TPI accommodate the weight of PM which might be useful in the cost sensitive application.  $T_{cd}$  and  $T_{mag}$  are calculated and presented in the graph in (Figure 6) and (Figure 7).

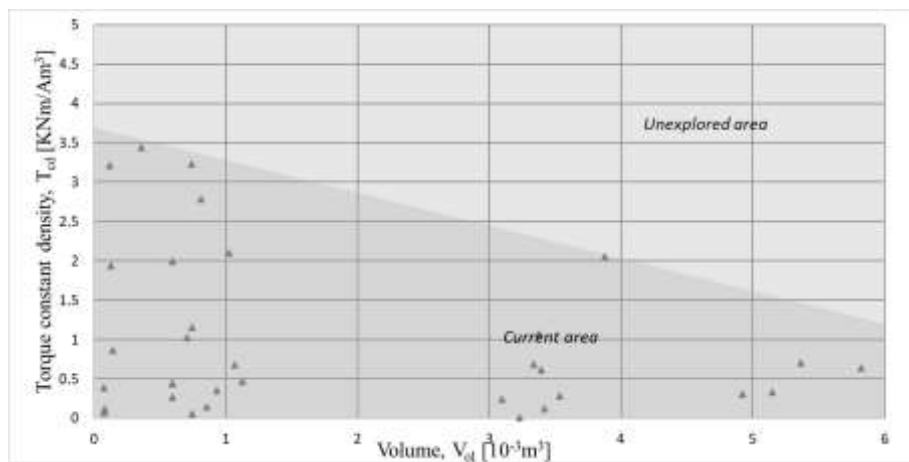


Figure 6. Torque constant density ( $T_{cd}$ ) versus volume (Vol) from past PMFSM publication.

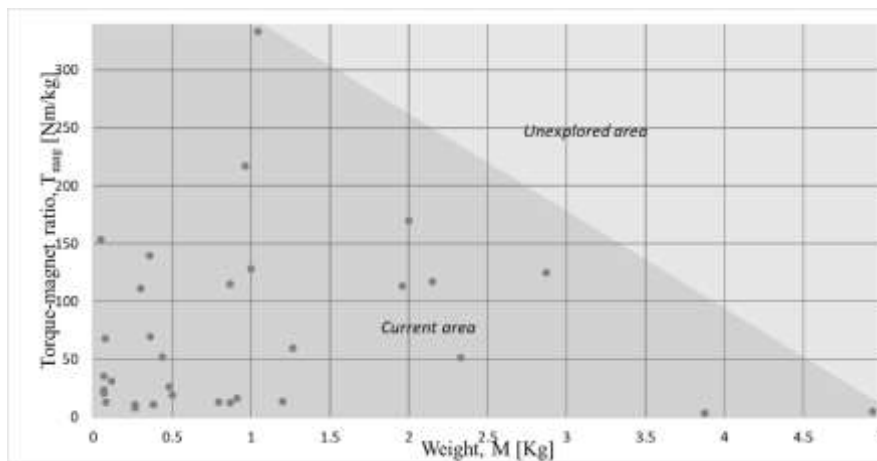


Figure 7. Torque-magnet ratio ( $T_{mag}$ ) versus magnet weight, (M) from past PMFSM publication.

$$T_{cd} = \frac{T}{Vol \cdot I \cdot ar} \tag{3}$$

$$T_{mag} = \frac{T}{Mag_{kg}} \tag{4}$$

### 3.3. Torque Normal Distribution

The distribution of each torque index are shown below (Figure 8-11). (Table 1) summarizes six best PMFSM design for each TPI. Motor output and the percentage of cogging torque were extracted as additional information for the reader. 3-phase outer rotor 12S-22P possess the highest torque density of 138KNm/m<sup>3</sup> but the torque-magnet ratio is low [10], and its torque ripple is 20%. On the other hand, 3-phase outer rotor 24S-14P produce high torque density and torque to magnet ratio but low torque constant and torque constant density which is suitable in various direct drive application [11–14]. Partition stator 12S-10P produce a good overall torque parameter for inner-rotor structure [15]. High torque constant density produce by 3-phase outer rotor 12S-22P is a trade-off of low torque to magnet ratio [16]. Full-pitch winding 12S-7P PMFSM is also listed in the table mainly because its inherit good winding factor [17]. Unfortunately, this design suffers a considerable unbalance magnetic field.

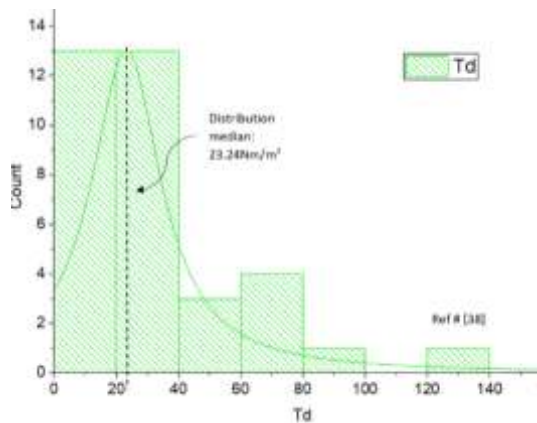


Figure 8. T<sub>d</sub> distribution of 35 designs

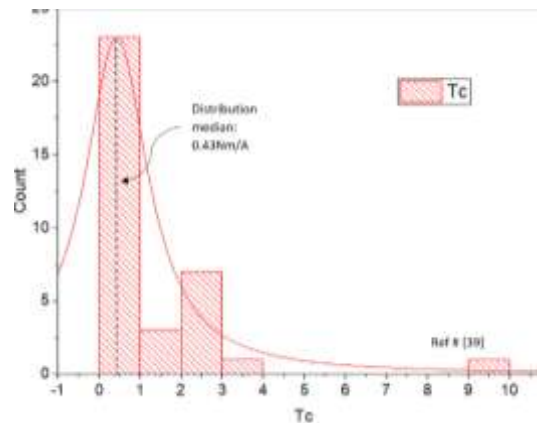


Figure 9. T<sub>c</sub> distribution of 35 designs.

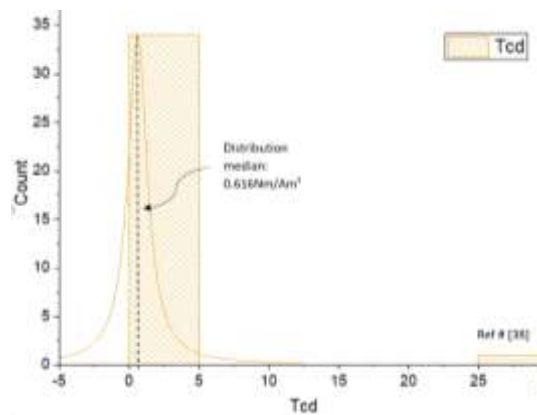


Figure 10. T<sub>cd</sub> distribution of 35 designs.

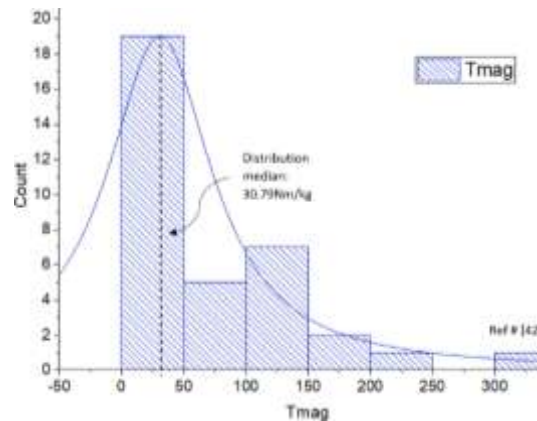


Figure 11. T<sub>mag</sub> distribution of 35 designs.

Table 1. Calculated torque parameter of six best PMFSM design

| Motor Type    | Vol 10 <sup>3</sup><br>m <sup>3</sup> | T <sub>d</sub><br>[KNm/m <sup>3</sup> ] | T <sub>c</sub><br>[Nm/A] | T <sub>cd</sub><br>[KNm/A.m <sup>3</sup> ] | T <sub>mag</sub><br>[Nm/kg] | *T <sub>cog</sub><br>[%] | Power<br>(kW) | Ref. |
|---------------|---------------------------------------|---|--------------------------|--|-----------------------------|--------------------------|---------------|------|
| Outer rotor   | 0.119                                 | <u>138.116</u>                          | 3.015                    | <u>25.412</u>                              | 13.658                      | 20                       | 4.13          | [10] |
| Outer rotor   | 5.362                                 | 38.975                                  | 0.410                    | 0.076                                      | <u>217.200</u>              | 4                        | 30            | [16] |
| Outer rotor   | 5.822                                 | 59.878                                  | 0.684                    | 0.117                                      | <u>333.647</u>              | 6                        | 45            | [14] |
| Outer rotor   | 4.919                                 | 69.095                                  | 0.429                    | 0.087                                      | 169.912                     | 1.5                      | 1.5           | [11] |
| Double stator | 3.878                                 | <u>92.318</u>                           | 1.432                    | 0.388                                      | 124.825                     | 8                        | 45            | [15] |
| Full Pitch    | 0.855                                 | 17.050                                  | 2.939                    | 3.437                                      | <u>16.013</u>               | 3                        | **0.9         | [17] |

\*Percentage ratio between cogging torque and average torque

\*\*Mechanical output

This state of the art graph in (Figure 4-6) in general do not show linearity between torque parameter and volume like expected in other machines [18, 19]. The main reason was the ratio of total volume to the magnet volume in a smaller motor is high hence elevated the torque produced thus it can vary widely over the full spectrum of the motor available [20]. Figure. 4(b) shows that the magnet weight is distributed randomly and at a maximum of near 5 kg. In general, the amount of output torque increase as either magnetic loading increase or electric loading increase. Designer should note that as magnetic loading increase, the flux weakening capability may become less effective. In terms of the economic evaluation of using PM machine over a non-PM machine, 25% of motor utilization over a year is enough to have 2.5 years of payback period [21]. The remaining data which were used to generate the graph were listed in (Table 2).

**Table 2.** Calculated torque parameter of the remaining 29 PMFSM design.

| Structure highlight                       | Vol.  | $T_d$<br>[KNm/m <sup>3</sup> ] | $T_c$<br>[Nm/A] | $T_{cd}$<br>[KNm/A.m <sup>3</sup> ] | $T_{mag}$<br>[Nm/kg] | Ref. |
|---|-------|--------------------------------|-----------------|-------------------------------------|----------------------|------|
| Conventional                              | 0.078 | 18.486                         | 0.048           | 0.616                               | 20.714               | [22] |
| Conventional                              | 0.077 | 32.216                         | 0.082           | 1.074                               | 35.286               | [22] |
| Conventional                              | 0.080 | 20.573                         | 0.055           | 0.686                               | 23.571               | [22] |
| Conventional                              | 0.081 | 20.460                         | 0.055           | 0.682                               | 23.571               | [22] |
| Conventional                              | 0.075 | 13.903                         | 0.035           | 0.473                               | 13.000               | [23] |
| Axial laminated                           | 0.359 | 20.909                         | 1.154           | 3.217                               | 153.583              | [24] |
| Five-Phase Modular                        | 3.393 | 3.978                          | 2.376           | 0.700                               | 3.486                | [25] |
| Five-Phase Modular                        | 3.373 | 3.617                          | 2.147           | 0.637                               | 3.150                | [25] |
| 3-Phase Outer rotor                       | 3.336 | 38.365                         | 1.109           | 0.332                               | 128.000              | [26] |
| 3-Phase Outer rotor                       | 1.067 | 46.855                         | 0.329           | 0.308                               | 139.471              | [27] |
| 3-Phase Outer rotor                       | 1.123 | 66.801                         | 2.301           | 2.048                               | 59.323               | [28] |
| 3-Phase Outer rotor                       | 5.146 | 23.243                         | 9.967           | 1.937                               | 51.362               | [11] |
| Partition stator                          | 0.129 | 39.908                         | 0.257           | 1.995                               | 68.015               | [29] |
| Partition stator double layer             | 0.594 | 6.823                          | 0.265           | 0.447                               | 10.631               | [30] |
| Partition stator single layer             | 0.594 | 6.722                          | 0.261           | 0.440                               | 10.473               | [30] |
| Partition stator doub. layer              | 0.594 | 3.622                          | 0.157           | 0.264                               | 8.062                | [30] |
| Partition stator single layer             | 0.594 | 4.852                          | 0.210           | 0.353                               | 10.799               | [30] |
| Alternate radial and circumferential flux | 0.933 | 10.182                         | 0.224           | 0.240                               | 19.000               | [31] |
| Conventional                              | 3.095 | 3.425                          | 0.021           | 0.007                               | 12.212               | [32] |
| 3 -phase                                  | 3.232 | 30.923                         | 0.196           | 0.061                               | 115.150              | [32] |
| V-shape magnet                            | 0.745 | 13.739                         | 0.858           | 1.152                               | 12.868               | [33] |
| Multi-tooth                               | 0.745 | 17.056                         | 0.643           | 0.863                               | 26.324               | [33] |
| Segmented magnet                          | 0.141 | 25.647                         | 0.144           | 1.026                               | 30.792               | [34] |
| Partition Rotor                           | 0.706 | 35.554                         | 2.282           | 3.232                               | 69.405               | [35] |
| Partition Rotor                           | 0.742 | 30.610                         | 2.064           | 2.783                               | 51.838               | [35] |
| Modular rotor                             | 0.812 | 41.016                         | 0.230           | 0.283                               | 111.000              | [36] |
| Segment. stator                           | 3.535 | 62.886                         | 0.437           | 0.124                               | 113.418              | [37] |
| Segment. stator                           | 3.417 | 73.825                         | 0.495           | 0.145                               | 117.473              | [38] |
| V-shape magnet inner stator               | 1.024 | 23.099                         | 2.150           | 2.100                               | 4.789                | [39] |

## 2. Conclusions

The data gathered to generate the graph are based on 35 designed published by the previous researcher specifically in PMFSM. The distribution median of torque density, torque constant, torque constant density and torque-magnet ratio are 23.24kNm/m<sup>3</sup>, 0.43Nm/A, 0.616kNm/Am<sup>3</sup> and 30.79Nm/kg respectively. Considering the presented information, the readers achieve enough understanding of the weaknesses and strong points of each PMFSM topology and its contribution towards the standardized indicator. According to this study, 4 out of 6 best design which yield the highest TPI are PMFSM using outer rotor structure. Each TPI value highlight torque ratio against

machine volume, armature current and magnet ratio. This information can be used to guide the machine designer to compare and compete based on the standardized values. There are still several factors that need to be investigated to improve the TPI calculation such as air gap, efficiency and torque ripple. Due to the limited information given in the literature, these parameters are not included in this paper.

### Acknowledgments

The authors would like to thank the editor and anonymous reviewers for their comments that help improve the quality of this work. The authors would like to thank the Ministry of Education Malaysia, Universiti Tun Hussein Onn Malaysia (UTHM) under Research Fund E15501 and Universiti Teknikal Malaysia Melaka (UTeM) for technical and financial support for this research.

### Authors' contributions

HA and SE carried out the study and wrote up the article. Both authors read and approved the final manuscript.

### Conflict of Interest

The authors confirm that there is no conflict of interest to declare for this publication.

### Refereneces

- [1]. Global EV Outlook 2018, OECD, 2018.
- [2]. López I., Ibarra E., Matallana A., Andreu J., Kortabarria I., Next generation electric drives for HEV/EV propulsion systems: Technology, trends and challenges, *Renew. Sustain. Energy Rev.*, 2019, 114:109336.
- [3]. AAB, Technical note - IEC 60034-30-1 standard on efficiency classes for low voltage AC motors, 2014.
- [4]. Miller J.F., Howell D., The EV everywhere grand challenge, *World Electr. Veh. J.*, 2013,
- [5]. Paulides J.J.H., Reluctance machines : facing the challenges of future electrical power trains, In: Presentation elektromagnetische-vermogenstechniek EMVT / Dutch Power, 2014.
- [6]. Pollock C., Wallace M., Flux switching motor, a DC motor without magnets or brushes, *Conf. Rec. - IAS Annu. Meet. (IEEE Ind. Appl. Soc.)*, 1999, 3:1980–1987.
- [7]. Pollock C., Pollock H., Uk L.E., Barron R., Sutton R., Coles J., *et al.*, Flux Switching Motors for Automotive Applications, 2003, 242–249.
- [8]. Firdaus Kashfi Raja Othman R.N., Zuki N.A.M., Ahmad S.R.C., Shukor F.A.A., Isa S.Z.M., Sulaiman E., *et al.*, Torque constant density in different type of double stator permanent magnet brushless DC motor, *Prog. Electromagn. Res. M*, 2018, 66:127–142.
- [9]. Trianni A., Cagno E., Accordini D., A review of energy efficiency measures within electric motors systems, *Energy Procedia*, 2019, 158:3346–3351.
- [10]. Kumar R., Sulaiman E., Soomro H.A., Musavi S.H.A., Kumar G., Sohu I.A., Electromagnetic analysis of outer rotor permanent magnet flux switching machine for downhole application, *ICIEECT 2017 - Int. Conf. Innov. Electr. Eng. Comput. Technol. 2017, Proc.*, 2017.
- [11]. Sulaiman E., Romalan G.M., Ghani N.W.A., Design improvement of flux switching permanent magnet using combined local and global method, *ICCEREC 2016 - Int. Conf. Control. Electron. Renew. Energy, Commun. 2016, Conf. Proc.*, 2017, 1:214–219.
- [12]. Ahmad M., Sulaiman E., Haron Z., Khan F., Mazlan M., Analysis of a New Dual Excitation Flux Switching Machine with Outer- Rotor Configuration for Direct Drive EV, 2015,



- 695:787–791.
- [13]. Sulaiman E. Bin, Arab A.M., Fundamental Study Of Outer-Rotor Hybrid Excitation Flux Switching Generator For Grid Connected Wind Turbine Applications, 2015 IEEE Student Conf. Res. Dev., 2015, 716–720.
- [14]. Mbadiwe E.I., Sulaiman E., Improved design of outer rotor machine in PM technology for motor bike drive application, In: ISCAIE 2018 - 2018 IEEE Symposium on Computer Applications and Industrial Electronics, 2018.
- [15]. Lee C.H.T., Kirtley J.L., Angle M., A Partitioned-Stator Flux-Switching Permanent-Magnet Machine with Mechanical Flux Adjusters for Hybrid Electric Vehicles, IEEE Trans. Magn., 2017, 53:1-7.
- [16]. Mbadiwe E., Sulaiman E., Flux switching permanent magnet motor using segmented outer rotor structure for electric scooter, Indones. J. Electr. Eng. Comput. Sci., 2017, 6:379–386
- [17]. Du Y., Zou C., Zhu X., Zhang C., Xiao F., A Full-Pitched Flux-Switching Permanent-Magnet Motor, IEEE Trans. Appl. Supercond., 2016, 26:1–5.
- [18]. Azhar F., Nasir N.A.M., Comparison and Prediction of Performance Index of Permanent Magnet Linear Motor, 2016 IEEE Int. Conf. Power Energy, 2016, 558–563.
- [19]. Azhar F., Wakiwaka H., Tashiro K., Nirei M., Design and Performance Index Comparison of the Permanent Magnet Linear Motor, 2015, 43:101–108.
- [20]. Aryanezhad M., Ostadaghaee E., A Novel Approach to Design the Dual Rotor Switched Reluctance Motor Based Electric Vehicles, 2015, 3:65–71.
- [21]. Adly A.A., Huzayyin A., The impact of demagnetization on the feasibility of permanent magnet synchronous motors in industry applications, J. Adv. Res., 2019, 17:103–108.
- [22]. Jusoh L.I., Sulaiman E., Kumar R., Bahrim F.S., Omar M.F., Preliminary studies of various rotor pole number for permanent magnet flux switching machines (PMFSM), Int. J. Appl. Eng. Res., 2017, 12:1377–1382.
- [23]. Jusoh L.I.B., Sulaiman E., Kumar R., Bahrim F.S., Design and performance of 8slot-12pole permanent magnet flux switching machines for electric bicycle application, Int. J. Power Electron. Drive Syst., 2017, 8:248–254.
- [24]. Xu W., Zhu J., Zhang Y., Guo Y., Lei G., New axial laminated-structure flux-switching permanent magnet machine with 6/7 poles, IEEE Trans. Magn., 2011, 47:2823–2826.
- [25]. Xue X., Zhao W., Zhu J., Liu G., Zhu X., Cheng M., Design of five-phase modular flux-switching permanent-magnet machines for high reliability applications, IEEE Trans. Magn., 2013, 49:3941–3944.
- [26]. Ahmad M.Z., Sulaiman E., Kosaka T., Analysis of high torque and power densities outer-rotor PMFSM with DC excitation coil for in-wheel direct drive, J. Magn., 2015, 20:265–272
- [27]. Fei W.Z., Shen J.X., Wang C.F., Luk P.C.K., Design and analysis of a new outer-rotor permanent-magnet flux-switching machine for electric vehicle propulsion, COMPEL - Int. J. Comput. Math. Electr. Electron. Eng., 2011, 30:48–61.
- [28]. Kumar R., Sulaiman E., Soomro H.A., Musavi S.H.A., Kumar G., Sohu I.A., Design and Investigation of Outer Rotor Permanent Magnet Flux Switching Machine for Downhole Application, Int. J. Power Electron. Drive Syst., 2017, 8:231–238.
- [29]. Khalidah S., Ahmad M.Z., Romalan G.M., Arap M.Z.M., Comparative analysis of double stator permanent magnet flux-switching machines with segmented inner stator and non-segmented inner stator, J. Telecommun. Electron. Comput. Eng., 2018, 10:37–41
- [30]. Awah C.C., Zhu Z.Q., Wu Z.Z., Zhan H.L., Shi J.T., Wu D., *et al.*, Comparison of Partitioned Stator Switched Flux Permanent Magnet Machines Having Single- or Double-Layer Windings, IEEE Trans. Magn., 2016, 52:1–4.
- [31]. Jenal M., Sulaiman E., Comparative study on a new permanent magnet flux switching machine configuration over segmental and salient rotor structure, ARPN J. Eng. Appl. Sci., 2015, 10:8846–8852.
- [32]. Othman S.M.N.S., Omar M.F., Rahimi S.K., Sulaiman E., Elementary analysis of segmental

- stator flux switching permanent magnet machine, *Int. J. Power Electron. Drive Syst.*, 2018, 9:972–978.
- [33]. Zhao G., Hua W., Comparative Study between a Novel Multi-Tooth and a V-Shaped Flux-Switching Permanent Magnet Machines, *IEEE Trans. Magn.*, 2019, 55:1–8.
- [34]. Al-Ani M.M.J., Jupp M.L., Switched flux permanent magnet machine with segmented magnets, In: 8th IET Conference Publications, 2016, 1–5.
- [35]. Xiang Z., Quan L., Zhu X., A New Partitioned-Rotor Flux-Switching Permanent Magnet Motor with High Torque Density and Improved Magnet Utilization, *IEEE Trans. Appl. Supercond.*, 2016, 26:1–5.
- [36]. Soomro I.A., Sulaiman E., Soomro H.A., Modular rotor Based Permanent Magnet Flux Switching Machine for Light Weight EV, In: Proceedings - 2019 IEEE 15th International Colloquium on Signal Processing and Its Applications, CSPA 2019, 2019.
- [37]. Bin Syed Othman S.M.N., Soomro H.A., Mbadiwe E.I., Bin Omar M.F., Sulaiman E. Bin, Design and analysis of three phase SegSta 12S-12P permanent magnet flux switching machine, 2019 2nd Int. Conf. Comput. Math. Eng. Technol. ICoMET 2019, 2019, 1–4.
- [38]. Othman S.M.N.B.S., Soomro H.A., Mbadiwe E.I., Omar M.F. Bin, Sulaiman E. bin, Design Optimisation of SegSta 12S-12P Permanent Magnet Flux Switching Machine, 2019 IEEE Int. Conf. Autom. Control Intell. Syst., 2019, 135–138.
- [39]. Zhu X., Shu Z., Quan L., Xiang Z., Pan X., Multi-Objective Optimization of an Outer-Rotor V-Shaped Permanent Magnet Flux Switching Motor Based on Multi-Level Design Method, *IEEE Trans. Magn.*, 2016, 52:1–8.